

An efficient acid hydrolysis of the ether bond assisted by the neighbouring benzamide group. Part 3^{1,2}

2 PERKIN

Antonio Arcelli,* Gianni Porzi,* Samuele Rinaldi and Sergio Sandri

Dipartimento di Chimica "G. Ciamician", Via Selmi 2, 40126 Università di Bologna, Italy.
E-mail: porzi@ciam.unibo.it

Received (in Cambridge, UK) 30th October 2000, Accepted 3rd January 2001

First published as an Advance Article on the web 23rd January 2001

The acid hydrolytic cleavage of **1** to **2**, assisted by a neighbouring benzamide group, was kinetically investigated in a wide range of HCl concentrations (1.67–8.7 M) and at various temperatures. Kinetic measurements were performed also in the presence of LiCl at constant ionic strength ($I = 5$ M). The rate determining step of the acid hydrolysis of **1** was recognized through the investigation of the acid catalyzed cyclization of **3** to **2**. Thermodynamic activation parameters were calculated and the experimental data discussed. The participation of the neighbouring benzamide group was evaluated to be about 7.3×10^3 .

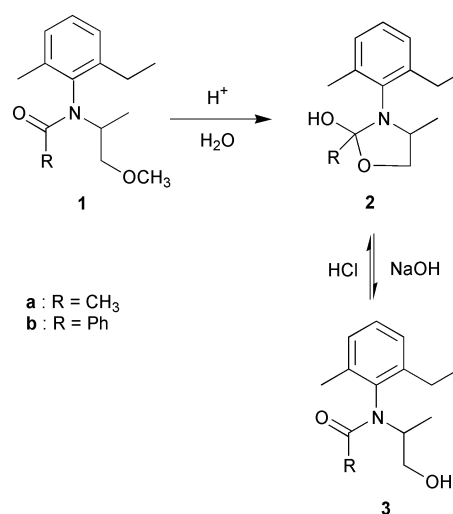
Introduction

We have previously investigated the acid hydrolysis of the methyl ether linkage of *N*-(2-ethyl-6-methylphenyl)-*N*-(1-methoxypropan-2-yl)acetamide (**1a**) assisted by the vicinal amide group.^{1,2} To the best of our knowledge the acid cleavage of a dialkyl ether intramolecularly assisted by an amide function has not previously been observed. The hypothesized mechanism involves two kinetically indistinguishable pathways.¹ In order to obtain further information about such assisted reactions and to investigate the influence of the acyl group on the reaction rate, we extended our study to the substrate *N*-(2-ethyl-6-methylphenyl)-*N*-(1-methoxypropan-2-yl)benzamide (**1b**). Thus, in this paper, the results of a kinetic investigation of the acid hydrolysis of **1b** to the oxazolidine derivative **2b**, easily converted to the open derivative **3b** (Scheme 1), are reported.

Results and discussion

The kinetic measurements were performed over a wide acidity range (1.67–8.7 M HCl) and at various temperatures (Table 1). The experimental data for the acid hydrolysis of **1b** at 71.2 °C, plotted in Fig. 1, show that the dependence of the pseudo first

order rate constant (k_{obs}) versus the HCl concentration is not linear, *i.e.* the hydrogen ion does not have a constant effect on the reaction rate, and at all the investigated temperatures the



Scheme 1

Table 1 Rate constants and experimental conditions for acid hydrolysis of **1b**

[HCl]/ mol dm ⁻³	10 ⁴ × $k_{\text{obs}}/\text{s}^{-1}$						
	45.4 °C	55.6 °C ^a	55.6 °C ^{b,c}	59.8 °C	66 °C	71.2 °C ^d	71.2 °C ^{b,e}
1.67			0.407			0.43	2.39
2.42	0.041	0.16	0.595		0.545	1.03	3.64
3.03	0.0714	0.26	0.743		0.984	1.58	4.09
				1.66 ^f		11.1 ^g	
4.01	0.169	0.58	0.973		2.24	3.47	5.70
4.70							6.47
4.92	0.35	1.13		1.85	3.9	6.4	
5.44						8.96	
5.90	0.808	2.28		4.10	7.39		
5.99						13	
6.59						17.5	
7.42	1.85	6.25		9.58	16.8	30.5	
8.70	3.25	10.40		15.5	27.90	47	

^a The slope calculated in the range 2.42–4.01 M HCl is $k_{\text{H}^+} = 2.62 \times 10^{-5} \text{ dm}^3 \text{ mol}^{-1} \text{ s}^{-1}$ ($r = 0.987$). ^b At $I = 5$ M (LiCl). ^c The slope is $k_{\text{H}^+} = 2.42 \times 10^{-5} \text{ dm}^3 \text{ mol}^{-1} \text{ s}^{-1}$ ($r = 0.987$). ^d The slope calculated in the range 1.67–4.01 M HCl is $k_{\text{H}^+} = 1.76 \times 10^{-4} \text{ dm}^3 \text{ mol}^{-1} \text{ s}^{-1}$ ($r = 0.976$). ^e The slope is $k_{\text{H}^+} = 1.34 \times 10^{-4} \text{ dm}^3 \text{ mol}^{-1} \text{ s}^{-1}$ ($r = 0.996$). ^f At 63.2 °C. ^g At 79.5 °C.

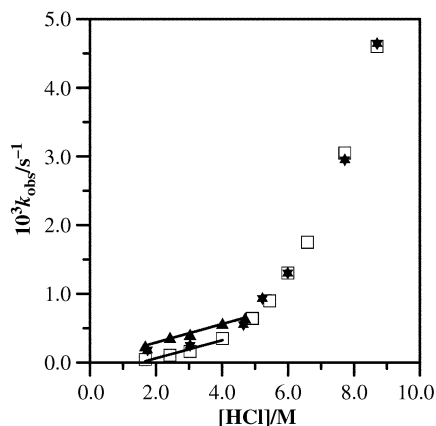


Fig. 1 Dependence of k_{obs} vs. $[\text{HCl}]$ at 71.2 °C for the hydrolysis of **1b** (\square), for the hydrolysis of **1b** at ionic strength $I = 5$ M with LiCl (\blacktriangle) and for the acid cyclization of **3b** (\star). Points are experimental and straight lines are calculated.

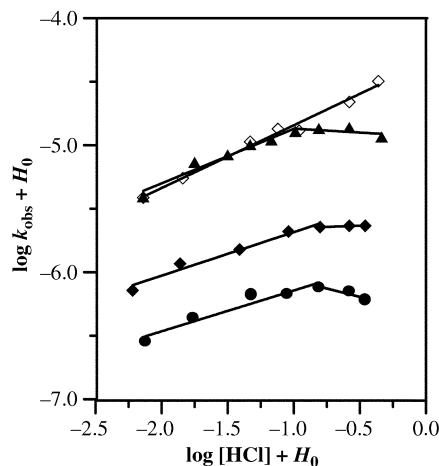


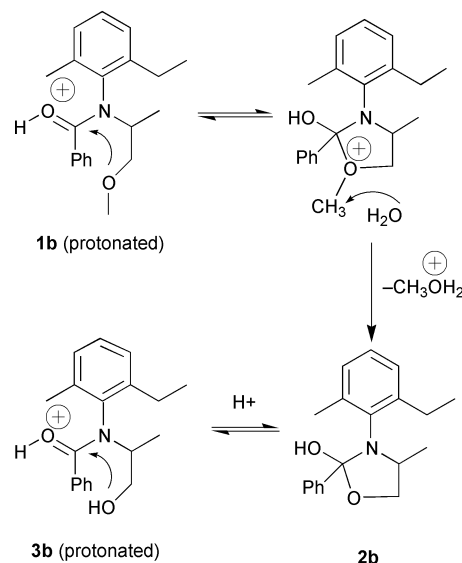
Fig. 2 Bunnett–Olsen plots of the acid hydrolysis of **1b** at 71.2 °C (\blacktriangle), at 55.6 °C (\blacklozenge), at 45 °C (\bullet) and of the acid cyclization of **3b** at 71.2 °C (\diamond). The straight lines are calculated.

plots evidence two distinct regions with different slopes (see Fig. 1). In actual fact, the k_{obs} steeply increases when the $[\text{HCl}]$ is raised from about 5 to 8.7 M, while the increase is smaller in the range 1.67–4.92 M HCl (see Fig. 1).

To explain these experimental data, we have elaborated the kinetic results by means of the Bunnett–Olsen treatment.³ As shown in Fig. 2, similar behaviours were obtained at different temperatures: straight lines of almost identical slopes (0.3–0.4) at high acidities, then a break and a second region, at low acidities, in which the slopes are close to zero or slightly negative.

The changes in the plot slopes could be interpreted as a consequence of: a) a change in the reaction mechanism or in the rate determining step, b) an inaccurate description of the substrate protonation, by means of the H_0 acidity function. For the acid hydrolysis of **1b** a mechanism different from that shown in Scheme 2 and already hypothesized for *N*-(2-ethyl-6-methylphenyl)-*N*-(1-methoxypropan-2-yl)acetamide (**1a**)¹ appears very unlikely.

On the other hand, it is unwise to take the Bunnett–Olsen criteria alone as evidence to ascertain a possible change in the reaction mechanism or rate determining step.^{4a} Therefore, in order to clarify the hydrolytic process, we thought it useful to investigate the substrate *N*-(2-ethyl-6-methylphenyl)-*N*-(1-hydroxypropan-2-yl)benzamide (**3b**) which in acid medium cyclizes to the oxazolidine derivative **2b** (Scheme 2). We believed the alcohol **3b** a suitable compound for providing very useful information about the rate determining step of the overall hydrolytic process of **1b**. In fact, the conversion of **1** into **2**

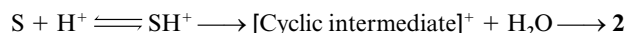


Scheme 2

involves two reaction steps (cyclization, then water attack), while in the conversion of **3** into **2** the process rate is given by the cyclization, the subsequent proton transfer being very fast.⁵ To this end kinetic measurements of the acid cyclization of **3b** to **2b** were carried out at 71.2 °C and we found that at $[\text{HCl}] > 5$ M the rate constants are very similar, or coincident, to those obtained for the acid hydrolysis of **1b** to **2b** (Fig. 1 and Tables 1, 2). This behaviour is consistent with the Bunnett–Olsen plot built for the cyclization of **3b** to **2b** which is linear in the whole acidity interval, the slope (0.5) being very similar to that found for the hydrolysis of **1b** at high acidity (Fig. 2). This result suggests that the first step in the acid hydrolysis of **1**, *i.e.* the cyclization to the oxonium ion, should be the rate determining step of the whole process. In this way, the different behaviour between **3b** and **1b** at low acidity could be due to the fact that the acidity function H_0 correctly describes the protonation of **3b**, but does not describe so well the substrate **1b**.

In favour of the mechanism hypothesized in Scheme 2 are the Molecular Electrostatic Potential (MEP) calculations showing that the preferential site of protonation for both the substrates **1b** and **3b** is the carbonyl oxygen. The geometries of the lowest energy conformers for both the substrates **1(a,b)** and **3(a,b)** were calculated by the AM1 semiempirical method (HyperChem Program, 1994) by using the “Polak-Ribiere” algorithm (RMS gradient 0.01 kcal).

The acid hydrolysis of the substrate **1** (depicted by S) to the cyclic product **2** can be schematized:



Since in our case the unprotonated species S is unreactive, the overall low rate can be expressed, according to the transition state theory,^{6a} by eqn. (1) where k_0 is the rate constant for the

$$k_{\text{obs}} = [k_0 / (K_{\text{SH}^+} + [\text{H}^+])] [\text{H}^+] f_{\text{SH}^+} / f^\ddagger \quad (1)$$

slow step, K_{SH^+} the dissociation constant for the protonated substrate, f_{SH^+} and f^\ddagger the activity coefficients of the protonated substrate and the transition state, respectively. Rearrangement of eqn. (1) yields eqn. (2).

$$k_{\text{obs}} = [k_0 [\text{SH}^+] / ([\text{S}] + [\text{SH}^+])] f_{\text{SH}^+} / f^\ddagger \quad (2)$$

If the substrate is essentially unprotonated stoichiometrically, *i.e.* $[\text{S}] \gg [\text{SH}^+]$, the expression (2) assumes the form given in eqn. (3) while when $[\text{S}] \ll [\text{SH}^+]$ eqn. (4) is applied.

Table 2 Rate constants and experimental conditions for acid cyclization of **3b** to **2b**

[HCl]/ mol dm ⁻³	10 ⁴ × <i>k</i> _{obs} /s ⁻¹					
	55.3 °C	59.8 °C	65.8 °C	68.4 °C	71.2 °C	79.1 °C
1.74					1.87	
3.03	0.348	0.63	1.37	1.72	2.35	5.51
4.65					5.53	
5.22					9.27	
5.99					13.7	
7.42	5.35		16	20.2	29.5	62.8
8.70					46.4	

Table 3 Thermodynamic activation parameters^{a,b} for acid hydrolysis of **1a**, **1b** and for cyclization of **3b** to **2b** at different conditions

Entry	[HCl]/mol dm ⁻³	Δ <i>G</i> [#] /kJ mol ⁻¹	Δ <i>H</i> [#] /kJ mol ⁻¹	Δ <i>S</i> [#] /J mol ⁻¹ K ⁻¹	<i>T</i> Δ <i>S</i> [#] /kJ mol ⁻¹
1a → 2a					
1	3.03 <i>I</i> = 5 M (LiCl)	110 ± 3	99 ± 2	-35 ± 6	-11 ± 2
2	7.42	109 ± 5	98 ± 4	-33 ± 11	-11 ± 4
1b → 2b					
3	3.03	112 ± 4	108 ± 3	-13 ± 8	-4 ± 2.5
4	4.92	109.5 ± 2	101 ± 1.5	-27 ± 4.5	-8.5 ± 1.5
5	7.42	106 ± 3	95 ± 2	-35 ± 6	-11 ± 2
6	8.70	105 ± 2	91 ± 1	-44 ± 4.5	-14 ± 1
7	3.03 <i>I</i> = 5 M (LiCl)	109.5 ± 5	106 ± 4	-11 ± 11	-3.5 ± 3.5
3b → 2b					
8	3.03	111.5 ± 3	108.5 ± 2	-9.5 ± 6	-3 ± 2
9	7.42	107 ± 3	97 ± 2	-30 ± 6	-10 ± 2

^a Obtained from $k_{\text{H}^+} = k_{\text{obs}}/[\text{H}^+]$. ^b Calculated at 50 °C from the equation $\ln k_{\text{H}^+} = \Delta S^\ddagger/R + \ln(kT/h) - E_a/RT$ plotting $\ln k_{\text{H}^+}$ vs. $1/T$ by means of a linear least square; standard errors are calculated according to ref. 7. ^c Calculated at 50 °C from $\Delta G^\ddagger = \Delta H^\ddagger - T\Delta S^\ddagger$. ^d Calculated at 50 °C from the equation $\Delta H^\ddagger = E_a - RT$.

$$k_{\text{obs}} = (k_0[\text{H}^+]/K_{\text{SH}^+}) f_{\text{SH}^+}/f^\ddagger \quad (3)$$

$$k_{\text{obs}} = k_0 f_{\text{SH}^+}/f^\ddagger \quad (4)$$

For the purpose of explaining the dependence of k_{obs} vs. [HCl] displayed in Fig. 1, in view of the above eqns. (1) or (2), the dissociation constant at 70 °C was measured and the value of $\text{p}K_{\text{SH}^+} = -2.6$ was obtained (see Experimental). Thus, this implies that at $H_0 > -1.6$ (*i.e.* [HCl] < 5 M) the substrate will be essentially unprotonated and therefore eqn. (3) can be applied. In the range $H_0 = -1.6$ to -2.75 (*i.e.* 5–8.7 M HCl), where appreciable quantities of both SH^+ and S exist in the pre-equilibrium mixture, eqn. (2) will be followed. At $H_0 < -3.6$ (*i.e.* [HCl] > 11.5 M) the substrate will be essentially protonated and eqn. (1) will reduce to eqn. (4).

From the plot reported in Fig. 1, in the range 1.67–4 M HCl a linear dependence of k_{obs} against HCl concentration can be observed, suggesting that on the basis of eqn. (3) the $f_{\text{SH}^+}/f^\ddagger$ ratio is almost constant. This observation is strengthened by the kinetic measurements conducted at various HCl concentrations in the presence of LiCl at constant ionic strength (*I*) in order to minimize the change in activity coefficients (Fig. 1). In fact, at *I* = 5 M in the range 1.67–4.7 M HCl a good linear plot was obtained according to the equation $k_{\text{obs}} = k_{\text{H}^+}[\text{H}^+] + k'$. The slope $k_{\text{H}^+} = 1.34 \times 10^{-4} \text{ dm}^3 \text{ mol}^{-1} \text{ s}^{-1}$ is the second-order rate constant (Table 1) and the intercept $k' = 2.09 \times 10^{-5} \text{ s}^{-1}$, about 30-fold smaller than k_{obs} measured at 1.67 M HCl, agrees with the not observed uncatalyzed competitive reaction. The similarity of this slope with that found in the absence of LiCl ($k_{\text{H}^+} = 1.76 \times 10^{-4} \text{ dm}^3 \text{ mol}^{-1} \text{ s}^{-1}$) in the same acidity range confirms that the $f_{\text{SH}^+}/f^\ddagger$ ratio remains practically constant. A divergent behaviour is shown in the rate–acidity profile at [HCl] > 5 M where the k_{obs} is not linearly dependent on the acidity, but it follows an apparently exponential trend. A reasonable explanation can be the following. Since, as reported

above, in the range 5–8.7 M HCl the k_{obs} depends on both the acidity and the $f_{\text{SH}^+}/f^\ddagger$ ratio [eqn. (1)], the latter has to increase considerably at [HCl] > 5 M, *i.e.* at higher ionic strengths. Really, the influence of the ion atmosphere on the $f_{\text{SH}^+}/f^\ddagger$ ratio should be larger at such high ionic strengths because intramolecular reaction occurs between a neutral-dipolar (-OCH₃) and a charged group (the protonated carbonyl).^{6b}

Thermodynamic activation parameters

As is well known, rather than the acidity function dependence such as the Bunnett–Olsen relationship, thermodynamic activation parameters are useful for providing further confirmatory evidence of the possible reaction mechanism.

The thermodynamic activation parameters for the acid catalyzed hydrolysis of **1b** to **2b** and cyclization of **3b** to **2b** were determined from the k_{obs} reported in Tables 1, 2, respectively. The values, evaluated from the linear relationship $\ln(k_{\text{obs}}/[\text{H}^+])$ vs. $1/T$, are reported in Table 3. The data obtained show that the decrease in free activation energy due to both an increase in HCl and the addition of LiCl is accompanied by an enthalpic advantage which exceeds the unfavourable entropy change. Since the investigated intramolecular reaction occurs between a charged and a dipolar group, the electrostatic contribution to the overall free activation energy is not relevant.^{6c} Really, the change in relative permittivity (by adding LiCl) does not significantly modify the ΔG^\ddagger : to this end compare entries 3, 4 and 7 in Table 3, taking into account that HCl and LiCl have a different molar depression of relative permittivity.⁸ Thus, we believe that the decrease in ΔG^\ddagger observed on going from 4.92 to 8.7 M HCl (entries 4, 5 and 6) can be ascribed to a significant increase in the $f_{\text{SH}^+}/f^\ddagger$ ratio [eqn. (1)].

As shown in Table 3, the thermodynamic activation parameters calculated for the acid cyclization of **3b** to **2b** (entries 8 and 9) are very similar, within experimental error, to those

Table 4 Rate constants and experimental conditions for acid hydrolysis of **1a**

[HCl]/ mol dm ⁻³	10 ⁴ × <i>k</i> _{obs} /s ⁻¹				
	50 °C	57.8 °C ^{a,b}	57.8 °C, <i>I</i> = 5 M (LiCl) ^c	69.9 °C	79.9 °C
1.67		0.026	0.596		
2.42		0.205	0.726		
3.03		0.382	0.894		
4.01		0.697	1.1		
7.42	1.1	2.86		11.3	26

^a In the range 1.67–4.01 M HCl the slope is $k_{H^+} = 2.9 \times 10^{-5} \text{ dm}^3 \text{ mol}^{-1} \text{ s}^{-1}$ ($r = 0.997$). ^b The k_{obs} measured in the range 4.75–8.37 M HCl are reported in ref. 1 and the respective slope is $k_{H^+} = 6.18 \times 10^{-5} \text{ dm}^3 \text{ mol}^{-1} \text{ s}^{-1}$ ($r = 0.994$). ^c The slope is $k_{H^+} = 2.2 \times 10^{-5} \text{ dm}^3 \text{ mol}^{-1} \text{ s}^{-1}$ ($r = 0.997$).

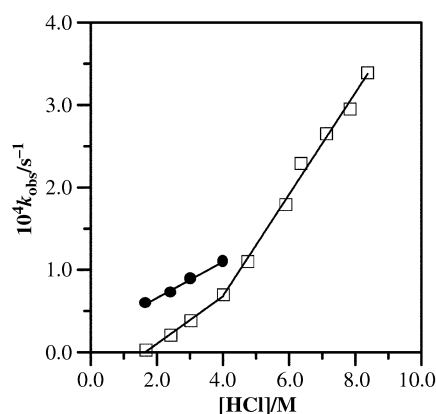


Fig. 3 Dependence of k_{obs} vs. [HCl] at 57.8 °C for the hydrolysis of **1a** (□) and for the hydrolysis of **1a** at ionic strength $I = 5 \text{ M}$ with LiCl (●). The values at [HCl] > 4.75 M are taken from the ref. 1. Points are experimental and straight lines are calculated.

obtained for the acid hydrolysis of **1b** to **2b** (entries 3 and 5) under the same conditions. This considerable similarity substantiates the above assertion that the rate determining step of the acid hydrolysis of **1** is its cyclization to the oxonium salt intermediate (Scheme 2): thus, in the HCl concentration range investigated, any change in the mechanism can be excluded.

Comparison between the substrates **1a** and **1b**

To better interpret the kinetic results we thought it may be helpful to compare the acid hydrolysis of **1b** and **1a**, the latter having been previously investigated¹ in the range 4.75–8.37 M HCl. To this end kinetic measurements of acid hydrolysis of **1a** were also performed in the range 1.67–4.01 M HCl at 57.8 °C (Table 4 and Fig. 3). The Bunnett–Olsen plot (not reported) built for **1a** showed a very similar behaviour to that observed for **1b**, with a breaking point that generates two slopes, 0.72¹ and 0.15. It is also interesting to note that the Bunnett–Olsen plot (not reported) built for the cyclization of *N*-(2-ethyl-6-methylphenyl)-*N*-(1-hydroxypropan-2-yl)acetamide (**3a**) is linear, the slope being 0.9, in the entire range of [HCl] investigated as found for **3b**.

The substrate **1a** was submitted to kinetic measurements also at ionic strength $I = 5 \text{ M}$ (LiCl) (Table 4 and Fig. 3).

The data obtained suggest some interesting considerations. In the range 1.67–4.01 M HCl at variable ionic strength, where the rate changes linearly with increasing [HCl], the slope, *i.e.* $k_{H^+} = 2.9 \times 10^{-5} \text{ dm}^3 \text{ mol}^{-1} \text{ s}^{-1}$, is comparable to $k_{H^+} = 2.2 \times 10^{-5} \text{ dm}^3 \text{ mol}^{-1} \text{ s}^{-1}$ found at $I = 5 \text{ M}$ (LiCl) (Table 4). In addition, these values are similar to those measured for the substrate **1b** ($k_{H^+} = 2.62 \times 10^{-5} \text{ dm}^3 \text{ mol}^{-1} \text{ s}^{-1}$) at 55.6 °C both in the absence and in the presence of LiCl (Table 1). These

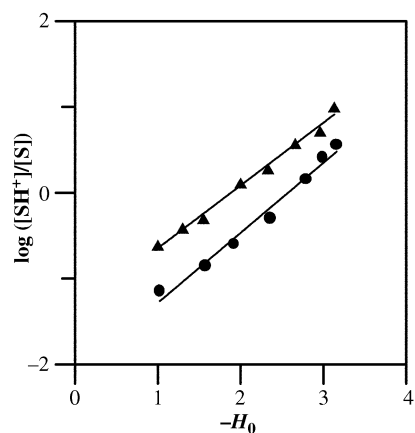


Fig. 4 Dependence of $\log ([\text{SH}^+]/[\text{S}])$ vs. H_0 for **1a** (▲) and for **1b** (●).

findings show that in the range 1–4 M HCl, analogously to that observed for **1b**, the ionic strength variation has a negligible effect on the reaction rate. From the $\text{p}K_{\text{SH}^+}$ value -1.9 , measured for **1a** at 60 °C (see Experimental), it can be deduced that in the range $H_0 = -0.9$ to -2.9 (*i.e.* 2.7–9.3 M HCl) appreciable quantities of both protonated and unprotonated substrate exist in the pre-equilibrium mixture. Then, in this range eqn. (2) should be followed, *i.e.* the profile of k_{obs} vs. acidity should be not linear, but rather resemble that observed for **1b** in the range 5–8.7 M HCl. Conversely, the rate–acidity profile is linear also at [HCl] > 4 M where, furthermore, the sensitivity of the rate to the medium acidity appears considerably smaller with respect to **1b**. This behaviour is difficult to interpret. Naively, for the substrate **1a** the acidity increasing, also at high ionic strength, causes a small change in the $f_{\text{SH}^+}/f^{\#}$ ratio.

These findings suggest that the unlike behaviour of two substrates at high acidity does not appear ascribable to the differences in the $\text{p}K_{\text{SH}^+}$ values, but more probably to the unequal effect of the ionic strength on the $f_{\text{SH}^+}/f^{\#}$ ratio of **1a** and **1b**.

The thermodynamic activation parameters calculated for **1a** at 3.03 M HCl and $I = 5 \text{ M}$ (LiCl), from data reported in Table 4, compare well with those obtained for **1b** under the same conditions (Table 3). The hydrolysis of **1a** and **1b** occurs with the same $\Delta G^{\#}$ though the former substrate requires a smaller $\Delta H^{\#}$ and a greater $\Delta S^{\#}$. The identical value (within experimental error) of free activation energy could be consistent with the similar stabilization of the two protonated reactants, considering that the transition states will probably be very similar in energy. In this regard, semi-empirical quantum mechanical calculations, performed by the AM1 method (from HyperChem program, 1994) allowed us to deduce that the positive charge of the protonated substrate **1b** is poorly delocalized because the aromatic ring is about 40° out of the carbonyl plane. Thus, on the protonated **1b** the weak spreading out of the charge over the phenyl ring will be comparable with that induced by the methyl group on the protonated **1a** through hyperconjugation.

In any case the data reported in the present work and in the previous paper¹ shows that the lowering in $\Delta G^{\#}$, with respect to the unassisted reaction,¹ is essentially due to an enthalpic gain. This is in agreement with a recent report⁹ that for ring sizes three through six the intramolecular reaction rate commonly depends on the enthalpic change occurring as the reactant structure is converted into the transition state.

Conclusions

Although some difficulties in interpreting experimental data have to be resolved (from both a chemical and mathematical point of view), the above mentioned findings allow the following conclusions.

For both substrates investigated, **1a** and **1b**, the mechanism involved is that reported in Scheme 2. In this way, the possible

alternative pathway proposed in the previous paper¹ can therefore be excluded.

The rate determining step is the cyclization of the protonated substrate, the subsequent attack of H₂O on the cationic cyclic intermediate being faster.

The substrates **1a** and **1b** show a very similar sensitivity to the acidity or to the ionic strength at values below 5 M, while at higher values the compound **1b** shows a remarkably greater sensitivity than **1a**. This behaviour does not appear ascribable to the different pK_{SH⁺} values (−1.9 and −2.6, respectively), but rather to a greater effect of the ionic strength on the $f_{SH^+}/f^{\#}$ ratio [eqn. (1)] for **1b** than **1a**.

The k_H values of hydrolysis of **1b** ($5.4 \times 10^{-4} \text{ dm}^3 \text{ mol}^{-1} \text{ s}^{-1}$, at 71.2 °C) and reference substrate¹ ($7.7 \times 10^{-8} \text{ dm}^3 \text{ mol}^{-1} \text{ s}^{-1}$, at 69.9 °C), allow us to estimate that the participation of the neighbouring benzamide group is about 7.3×10^3 . This value is lowered to about 3×10^3 by comparison with diethyl ether. In fact, the polar effect of the protonated amino-ether of the unassisted model can be estimated as 2.5-fold.¹

In conclusion, in order to achieve a more satisfactory solution to the complex problem about the influence of the acidity and ionic strength on the reaction rate, further investigation is in progress providing additional and useful data especially on the salt effects.

Experimental

General

¹H- and ¹³C-NMR spectra were recorded with a Varian Gemini 300 (300 MHz) instrument by using CDCl₃ as solvent. UV spectra and kinetic measurements were recorded on a Perkin-Elmer Lambda 6 spectrophotometer.

Synthesis of *N*-(2-ethyl-6-methylphenyl)-*N*-(1-methoxypropan-2-yl)benzamide (**1b**)

It was obtained by treating the *N*-(2-ethyl-6-methylphenyl)-*N*-(1-hydroxypropan-2-yl)amine [¹H-NMR δ 1.07 (d, 3H, $J = 6.5$ Hz), 1.25 (t, 3H, $J = 7$ Hz), 2.3 (s, 3H), 2.45–2.75 (m, 4H), 3.36 (m, 1H), 3.5 (dd, 1H, $J = 6.8, 11$ Hz), 3.69 (dd, 1H, $J = 4.1, 11$ Hz), 6.85–7.1 (m, 3ArH)], synthesized starting from 6-ethyl-*o*-toluidine and (±)-ethyl 2-bromopropionate followed by lithium borohydride reduction, with an equivalent amount of NaH (80% dispersion in mineral oil) under an inert atmosphere. After about 2 h, CH₃I (1.5 equivalent) was added dropwise and the reaction mixture stirred for about 4 h at rt. The crude reaction product [¹H-NMR δ 1.21 (d, 3H, $J = 6.7$ Hz), 1.26 (t, 3H, $J = 7.6$ Hz), 2.31 (s, 3H), 2.68 (q, 1H, $J = 7.6$ Hz), 3.37 (m, 7H), 6.9 (m, 1ArH), 7.05 (m, 2ArH)] was isolated and reacted in CHCl₃ with benzoyl chloride in the presence of triethylamine. The reaction mixture was refluxed for about 8 h and worked up by the usual procedure. After purification by silica gel chromatography eluting with hexane–ethyl acetate, the pure product was isolated as an oil in 70% overall yield. ¹H-NMR δ 1.13 (2t, 3H, $J = 7.5$ Hz), 1.38 (2d, 3H, $J = 6.7$ Hz), 2.28 (s, 3H), 2.58 (2m, 2H), 3.33 (2s, 3H), 3.79 (m, 1H), 3.97 (m, 2H), 7.1 (m, 8ArH); ¹³C-NMR δ 13.6, 13.8, 15.4, 15.6, 19.3, 19.5, 23.7, 57.6, 58.7, 75.1, 75.3, 126.2, 127.3, 127.7, 127.8, 128.5, 129.7, 135.9, 136.1, 136.5, 140.6, 141.5, 141.6, 170.9.

Synthesis of 3-(2-ethyl-6-methylphenyl)-2-hydroxy-4-methyl-2-phenyloxazolidine (**2b**)

It was obtained by submitting **1b** to hydrolysis in 5 M HCl at 80 °C for at least 2 h. The reaction solution was then evaporated to dryness *in vacuo* and the oily residue was pure by TLC analysis. ¹H-NMR δ 1.12 (t, 3H, $J = 7.5$ Hz), 1.18 (t, 3H, $J = 7.5$ Hz), 1.47 (2d, 3H, $J = 6.7$ Hz), 2.28 (2s, 3H), 2.55 (m, 2H), 3.95 (m, 1H), 4.12 (m, 2H), 7.15 (m, 8ArH); ¹³C-NMR δ 13.6, 13.8, 14.6, 14.9, 19.1, 19.4, 23.6, 46.8, 47.0, 60.3, 60.4, 126.5,

127.3, 127.7, 127.8, 128.0, 128.7, 128.8, 130.0, 135.4, 135.5, 140.2, 141.1, 170.9.

Synthesis of *N*-(2-ethyl-6-methylphenyl)-*N*-(1-hydroxypropan-2-yl)benzamide (**3b**)

The acid aqueous solution of **2b** was made alkaline with NaOH, then extracted with ethyl acetate. The oil product, recovered after total evaporation *in vacuo* of the organic solvent, was pure by the TLC analysis. ¹H-NMR δ 1.15 (2t, 3H, $J = 7.5$ Hz), 1.47 (2d, 3H, $J = 7.1$ Hz), 2.3 (2s, 3H), 2.52 (m, 1H), 2.68 (m, 1H), 3.85 (m, 2H), 4.16 (m, 1H), 4.8 (m, OH), 7.15 (m, 8ArH); ¹³C-NMR δ 13.7, 14.0, 19.2, 19.4, 23.6, 23.7, 62.0, 62.2, 66.3, 126.6, 126.7, 127.4, 127.9, 128.0, 128.9, 130.1, 135.3, 135.8, 141.0, 172.5. IR (thin film): $\nu = 1626$ (C=O), 3430 cm^{−1} (OH).

pK_{SH⁺} measurements

The pK_{SH⁺} measurements of **1a** and **1b** were performed spectrophotometrically in HCl solutions. Samples were prepared by adding 30 μ L of a stock solution of **1a** (0.11 M in MeOH) and **1b** (9.8×10^{-3} M in MeOH) at 3 mL of acid solution thermostatted at 60 and 70 °C, respectively. The optical density (OD) was monitored at $\lambda = 266$ nm for **1a** and at $\lambda = 258$ nm for **1b**. The OD value of unprotonated **1a** was evaluated in aqueous alcoholic solutions (1–2 M HCl–MeOH = 2:1), the product being insoluble in low HCl concentration. The addition of MeOH does not produce spectral change. Since at HCl > 5 M the hydrolysis of **1b** proceeds significantly, the absorbance was recorded as function of time and it was extrapolated to $t = 0$. The OD values of protonated **1a** and **1b** species were measured in 9–11 M H₂SO₄ because concentrated HCl does not allow total protonation. The absorbances at the λ employed did not change when H₂SO₄ instead of HCl was used. In addition, owing to the medium effects, the OD values of protonated and unprotonated **1b** were estimated by using the Katritzky method.¹⁰ Sigmoid curves of OD vs. H_0 (values corrected at 60 °C for **1a** and extrapolated to 70 °C for **1b**)^{4b,c} were obtained.

The linear plots of $\log ([SH^+]/[S])$ against H_0 are reported in Fig. 4. The pK_{SH⁺} values, calculated from the equation $pK_{SH^+} = H_0 + n \log ([SH^+]/[S])$, are: -1.9 ± 0.15 ($n = 0.73$) for **1a** and -2.6 ± 0.20 ($n = 0.82$) for **1b**.

Kinetic experiments

The kinetic measurements of acid catalysed hydrolysis of **1a** (Table 4) were followed as described in ref. 1. The hydrolysis of **1b** was investigated at various temperatures, in a large range of HCl concentrations (1.0–8.7 M) and in the presence of LiCl (Table 1). The reaction was followed spectrophotometrically by measuring the change in the OD at $\lambda = 258$ nm. 30 μ L of the stock solution of **1b** (0.02 M in MeOH) were added to 3 mL of HCl thermostatted in a 1 cm path cell of the spectrophotometer. The pseudo first order rate constants (k_{obs}) were obtained from the equation $OD = OD_{\infty} + (OD_{\infty} - D_0) \times [1 - \exp(-t \times k_{obs})]$ by plotting at least 200 values of OD with a non-linear last square routine (FigP6.0 programme by Biosoft). Excellent plots were obtained with correlation coefficients above 0.999. OD_∞ values were taken after at least ten half lives. In all cases investigated the reaction followed a first order over at least 90% of reaction.

After completion of the reaction, about ten half lives at 66 °C, the compound **3b**, isolated by alkalization, was the sole reaction product and it was identified by its ¹H-NMR spectrum (see above). The structure of the cyclic product **2b** was deduced from the ¹H-NMR spectrum, as previously reported for the analogous *N*-(2-ethyl-6-methylphenyl)-*N*-(1-methoxypropan-2-yl)acetamide (**1a**).¹

The kinetics of acid catalysed cyclization of **3b** to **2b** were followed spectrophotometrically (at $\lambda = 258$ nm) at 3.03 and 7.42 M HCl and at various temperatures (Table 2).

Acknowledgements

Financial support from the University of Bologna (Funds for selected research topics and Fondi Ricerca Istituzionale, ex 60%).

References

- 1 A. Arcelli, G. Porzi and S. Sandri, *Tetrahedron*, 1995, **51**, 9729 and references therein.
- 2 A. Arcelli, M. Papa, G. Porzi and S. Sandri, *Tetrahedron*, 1997, **53**, 10513.
- 3 T. H. Lowry and K. Schueller Richardson, *Mechanism and Theory in Organic Chemistry*, Harper and Row, New York, 1987, p. 259.
- 4 (a) C. H. Rochester, *Acidity Functions*, Academic Press, London, 1970, p. 194; (b) C. H. Rochester, *Acidity Functions*, Academic Press, London, 1970, p. 39; (c) C. H. Rochester, *Acidity Functions*, Academic Press, London, 1970, p. 28.
- 5 M. Eigen, *Angew. Chem., Int. Ed. Engl.*, 1964, **3**, 1.
- 6 (a) C. H. Bamford and C. F. H. Tipper, *Comprehensive Chemical Kinetics*, Elsevier, New York, 1969, vol. 2, p. 310; (b) C. H. Bamford and C. F. H. Tipper, *Comprehensive Chemical Kinetics*, Elsevier, New York, 1969, vol. 2, p. 333; (c) C. H. Bamford and C. F. H. Tipper, *Comprehensive Chemical Kinetics*, Elsevier, New York, 1969, vol. 2, p. 323.
- 7 L. L. Schaleger and F. A. Long, *Adv. Org. Chem.*, 1963, **1**, 1.
- 8 R. A. Robinson and R. H. Stokes, *Electrolyte Solutions*, Butterworths, London, 1959, p. 18.
- 9 F. C. Lightstone and T. C. Bruice, *Bioorganic Chemistry*, 1998, **26**, 193.
- 10 A. R. Katritzky, A. J. Waring and K. Yates, *Tetrahedron*, 1963, **19**, 465.